

Structure and Dynamics of $[\text{Nb}(\eta^5\text{-C}_5\text{H}_4\text{SiMe}_3)_2(\eta^2\text{-H}_2\text{BR}_2)]$ ($\text{R}_2 = \text{O}_2\text{C}_6\text{H}_4$, C_8H_{14} , H_2) Complexes. A Combined Experimental and Theoretical Study

Antonio Antiñolo,[†] Fernando Carrillo-Hermosilla,[†] Juan Fernández-Baeza,[†]
Santiago García-Yuste,[†] Antonio Otero,^{*,†} Ana María Rodríguez,[†]
Javier Sánchez-Prada,[†] Elena Villaseñor,[†] Ricard Gelabert,[‡] Miquel Moreno,[‡]
José M. Lluch,^{*,‡} and Agustí Lledós^{*,‡}

Departamento de Química Inorgánica, Orgánica y Bioquímica, Facultad de Ciencias Químicas, Universidad de Castilla-La Mancha, Campus Universitario de Ciudad Real, 13071-Ciudad Real, Spain, and Departament de Química, Universitat Autònoma de Barcelona, 08193 Bellaterra, Barcelona, Spain

Received March 13, 2000

Dihydrogen elimination from the reaction of the niobocene trihydride $\text{Cp}'_2\text{NbH}_3$ ($\text{Cp}' = \eta^5\text{-C}_5\text{H}_4\text{SiMe}_3$) and the appropriate borane provides a synthetic route to the new borate-containing niobocene complexes $[\text{Nb}(\eta^5\text{-C}_5\text{H}_4\text{SiMe}_3)_2(\eta^2\text{-H}_2\text{BR}_2)]$ ($\text{R}_2 = \text{O}_2\text{C}_6\text{H}_4$ (**1**), C_8H_{14} (**2**), H_2 (**3**)). The reaction with $\text{H}_2\text{BO}_2\text{C}_6\text{H}_4$ or $\text{H}_2\text{BC}_8\text{H}_{14}$ proceeds at mild temperature, and the $\text{BH}_3\cdot\text{THF}$ adduct reacts even at low temperature. Complexes **2** and **3** show dynamic behavior in solution. Spectroscopic and theoretical studies were carried out in order to clarify these dynamic processes. In addition, X-ray diffraction studies of **2** were carried out and the results correlated with the theoretical data. Finally, reactions of $\text{Cp}'_2\text{Nb}(\text{H})(\text{L})$ ($\text{L} = \text{CO}$, $\text{CN}(\text{2,6-Me}_2\text{C}_6\text{H}_3)$, $\text{tBuOOCH}=\text{CHCOO}^t\text{Bu}$) with $\text{BH}_3\cdot\text{THF}$ give rise to the complex **3**, with the elimination of the appropriate ancillary ligand L.

1. Introduction

Transition-metal complexes with boron ligands are receiving renewed interest because of their practical applications in synthesis and catalysis and also because their structure and bonding constitute a compelling topic in transition-metal chemistry. A boron-containing species can be coordinated to a transition metal as a borate, boryl, or neutral borane ligand. Many tetrahydroborate¹ and organohydroborate² metal complexes have been prepared and studied. The synthesis and characterization in the last few years of several σ complexes³ have expanded the structural possibilities for boron ligands with B–H bonds. Borane σ complexes, with coordination of the B–H bond of a neutral borane to a transition-metal center, have been recently reported.^{4,5} Mechanistic studies have revealed that borane σ complexes can be intermediates in catalytic hydroboration processes.⁶ The chemistry of transition-metal boryl

compounds has been pursued because of their importance in the metal-mediated functionalization of organic molecules, such as alkenes, alkynes, dienes, or ketones, by boron reagents.⁷ The synthesis⁸ of these compounds habitually implies reactions between (i) anionic metal species and haloboranes, (ii) metal halide complexes and borate salts, (iii) metal hydride complexes and hydrido-boranes or haloboranes, by oxidative addition, and (iv), more recently, reactions between hydrideolefin complexes and hydridoboranes.

Early-transition-metal complexes with metal–boron bonds constitute an interesting field of research in this area because of the wide variety of structural situations found in these complexes, from hydroborate and boryl derivatives to agostic B–H–M interactions. Special interest has been focused on metallocene derivatives of group 5.^{9–13} In this respect, complexes of the type

* To whom correspondence should be addressed.

[†] Universidad de Castilla-La Mancha.

[‡] Universitat Autònoma de Barcelona.

(1) (a) Marks, T. J.; Kolb, J. R. *Chem. Rev.* **1977**, *77*, 263. (b) Lin, Z.; Xu, Z. *Coord. Chem. Rev.* **1996**, *156*, 139.

(2) (a) Liu, J.; Meyers, E. A.; Shore, S. G. *Inorg. Chem.* **1998**, *37*, 496. (b) Liu, F.-C.; Liu, J. M.; Meyers, E. A.; Shore, S. G. *Inorg. Chem.* **1998**, *37*, 3293.

(3) (a) Kubas, G. J. *Acc. Chem. Res.* **1988**, *21*, 120. (b) Crabtree, R. H. *Angew. Chem., Int. Ed. Engl.* **1993**, *32*, 789.

(4) (a) Hartwig, J. F.; Muhoro, C. N.; He, X.; Eisenstein, O.; Bosque, R.; Maseras, F. *J. Am. Chem. Soc.* **1996**, *118*, 10936. (b) Muhoro, C. N.; Hartwig, J. F. *Angew. Chem., Int. Ed. Engl.* **1997**, *36*, 1510. (c) Muhoro, C. N.; He, X.; Hartwig, J. F. *J. Am. Chem. Soc.* **1999**, *121*, 5033.

(5) (a) Macias, R.; Rath, N. P.; Barton, L. *Angew. Chem., Int. Ed.* **1999**, *38*, 162. (b) Shimoi, M.; Nagai, S.; Ichikawa, M.; Kawano, Y.; Katoh, K.; Uruichi, M.; Ogino, H. *J. Am. Chem. Soc.* **1999**, *121*, 11704.

(6) Hartwig, J. F.; Muhoro, C. N. *Organometallics* **2000**, *19*, 30.

(7) Burgess, K.; Ohlmeyer, M. J. *Chem. Rev.* **1991**, *91*, 1179.

(8) Irvine, G. J.; Lesley, M. J. G.; Marder, T. B.; Norman, N. C.; Rice, C. R.; Robins, E. G.; Roper, W. R.; Whittell, G. R.; Wright, L. J. *Chem. Rev.* **1998**, *98*, 2685.

(9) (a) Lucas, C. R.; Green, M. L. H. *J. Chem. Soc., Chem. Commun.* **1972**, 1005. (b) Kurilova, N. I.; Gusev, A. I.; Struchkov, Y. T. *Zh. Strukt. Khim.* **1974**, *15*, 718. (c) Marks, T. J.; Kennelly, W. J. *J. Am. Chem. Soc.* **1975**, *97*, 1439. (d) (a) Bell, R. A.; Cohen, S. A.; Doherty, N. M.; Threlkel, R. S.; Bercaw, J. E. *Organometallics* **1986**, *5*, 972.

(10) Green, M. L. H.; Wong, L. L. *J. Chem. Soc., Dalton Trans.* **1989**, 2133.

(11) (a) Lantero, D. R.; Motry, D. H.; Ward, D. L.; Smith, M. R., III. *J. Am. Chem. Soc.* **1994**, *116*, 10811. (b) Lantero, D. R.; Miller, S. L.; Cho, J. Y.; Ward, D. L.; Smith, M. R., III. *Organometallics* **1999**, *18*, 235.

(12) Hartwig, D. F.; De Gala, S. R. *J. Am. Chem. Soc.* **1994**, *116*, 3661.

(13) Lantero, D. R.; Ward, D. L.; Smith, M. R., III. *J. Am. Chem. Soc.* **1997**, *119*, 9699.

Cp₂M(H₂BR₂) (Cp = C₅H₅, C₅Me₅; M = Nb, Ta; H₂BR₂ = H₂BH₂,^{9,10} H₂BO₂C₆H₄,^{11,12} H₂BO₂C₆H₃-4-^tBu,¹³ H₂BO₂-C₆H₃-3-^tBu,¹³ H₂BC₈H₁₄)¹² have been prepared.

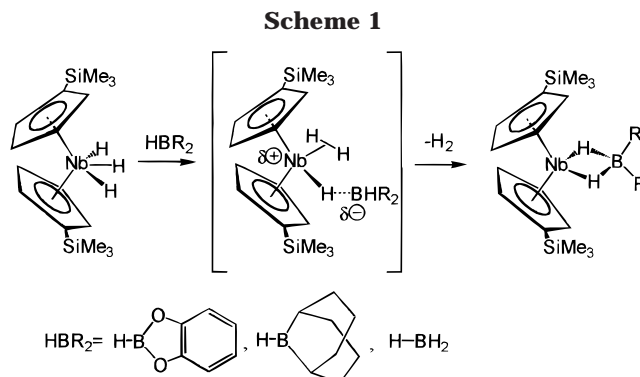
A new bonding possibility can arise when the metal center also supports hydride ligands. Recently, the ability of M–H bonds to act as an electron pair donor to a trivalent boron to form a hydrogen-bridged bond, which had been suggested,¹⁴ has been confirmed by theoretical calculations¹⁵ and experimentally demonstrated.¹⁶ Actually, the bonding in early-transition-metal complexes containing transition-metal–boron interactions and hydrides was described as an equilibrium between boryl, hydridoborate, and hydride/borane structures.¹²

Lately, theoretical studies have suggested the possibility that the interaction between metallocene trihydrides and HBR₂ species can have interesting applications in the chemistry of these systems, such as the formation and elimination of dihydrogen from these complexes.¹⁷ We have further explored the synthetic potentialities of the niobocene trihydride/borane interaction. Herein we report the preparation and spectroscopic characterization of three new substituted niobocene complexes containing boron ligands, Cp'₂Nb(η^2 -H₂BO₂C₆H₄) (**1**), Cp'₂Nb(η^2 -H₂BC₈H₁₄) (**2**), and Cp'₂Nb(η^2 -H₂BH₂) (**3**), where Cp' = η^5 -C₅H₄SiMe₃. Analogous compounds with Cp instead of Cp' were previously reported.^{9–12} However, the presence of SiMe₃ in the Cp ring leads to the possibility of a more in-depth ¹H NMR study as a consequence of the different hydrogen atoms of the Cp rings being inequivalent. The temperature-variable ¹H NMR study of **2** and **3** has shown a dynamic behavior of both systems in solution. The molecular structure of **2** has been established by X-ray diffraction studies. Moreover, theoretical calculations have been used to explain the structural features of both complexes and to explain the temperature dependence of their ¹H NMR spectra.

2. Results and Discussion

2.1. Synthesis. The complexes Cp'₂Nb(η^2 -H₂BO₂C₆H₄) (**1**) and Cp'₂Nb(η^2 -H₂BC₈H₁₄) (**2**) were prepared by addition of catecholborane or 9-borabicyclononane, respectively, to a toluene solution of the trihydride niobocene Cp'₂Nb(H)₃,¹⁸ at 40 °C (see Scheme 1).

No reaction between Cp'₂Nb(H)₃ and the aforementioned borane reagents has been observed at room temperature. Conversely, with stronger Lewis acids such as B(C₆F₅)₃ the reaction between the trihydride niobocene and the Lewis acid was completed even at low temperatures, as pointed out by several of us elsewhere.¹⁹ In accordance with this noted reactivity, Cp'₂Nb(η^2 -BH₄) (**3**) was instantaneously obtained in



quantitative yield by reaction of a toluene solution of Cp'₂Nb(H)₃ and BH₃·THF at –78 °C, due to the Lewis acid character being stronger than that of catecholborane or 9-borabicyclononane. Previously, the reactions of Cp'₂Nb(H)₃ with these latter boranes have been described, which take place at 65 and 20 °C, respectively.¹² It is also noteworthy that the complex Cp'₂Nb(H)₃ loses dihydrogen in the absence of a Lewis acid at 80 °C.²⁰

The mechanism proposed for the process (see Scheme 1) can be explained in terms of the interaction between BHR₂ (R₂ = O₂C₆H₄, C₈H₁₄, H₂), a Lewis acid, and one of the hydride ligands of Cp'₂Nb(H)₃, followed by H₂ elimination. In this latter process, the strength of the Lewis acid is directly related to the height of the energy barrier for the H₂ loss, as was theoretically proposed by some of us.^{15,17} In fact, we demonstrated by means of DFT calculations that the interaction of a Lewis acid with the lateral hydride of a trihydride isomer causes the depletion of electron density on the metal center and stabilizes a dihydrogen structure. The presence of a Lewis acid assists in the subsequent dihydrogen elimination.

To gain more insight into the hydride–BH₃ interaction, the reaction of BH₃·THF with several hydrido-niobocene complexes, namely Cp'₂Nb(H)(L) (L = CO, CN(2,6-Me₂C₆H₃), ^tBuOOCH=CHCO^tBu),²¹ was also considered. The corresponding adducts [Cp'₂Nb(BH₄)(L)] were not detected or isolated. However, the reaction at room temperature gave rise to the formation of **3** and the corresponding elimination of the ancillary ligand (see Scheme 2). In the case where L = olefin, a temperature of 40 °C was necessary to eliminate the olefin and give the borate complex **3**, probably because of the considerable metallocyclopropane character of the initial complex.^{21c}

2.2. Structure and Dynamics. Complexes **1–3** have been studied by means of ¹H and ¹³C NMR spectroscopy. In some cases, coalescence of signals in the NMR spectra has been discovered, a situation that indicates the existence of dynamic processes. Further theoretical studies have been carried out in order to clarify the mechanism of these processes. Structural information has been obtained by means of an X-ray diffraction study of **2**.

(14) Baker, R. T.; Ovenall, D. W.; Calabrese, J. C. *J. Am. Chem. Soc.* **1990**, *112*, 9399.

(15) Camanyes, S.; Maseras, F.; Moreno, M.; Lledós, A.; Lluch, J. M.; Bertrán, J. *Angew. Chem., Int. Ed. Engl.* **1997**, *36*, 265.

(16) Liu, F.-C.; Liu, J.; Meyers, E. A.; Shore, S. G. *Inorg. Chem.* **1999**, *38*, 2169.

(17) Camanyes, S.; Maseras, F.; Moreno, M.; Lledós, A.; Lluch, J. M.; Bertrán, J. *J. Chem. Eur. J.* **1999**, *5*, 1166.

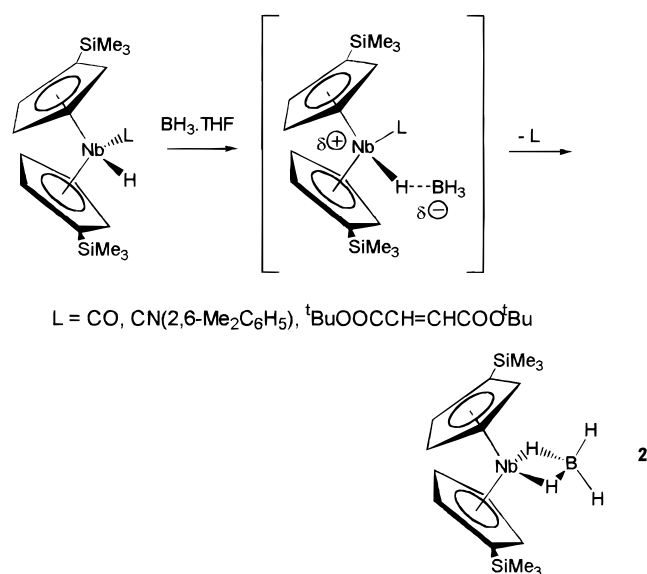
(18) Antiñolo, A.; Chaudret, B.; Commenges, G.; Fajardo, M.; Jalón, F.; Morris, R. H.; Otero, A.; Schweitzer, C. T. *J. Chem. Soc., Chem. Commun.* **1988**, 1210.

(19) Antiñolo, A.; Carrillo-Hermosilla, F.; Fernández-Baeza, J.; García-Yuste, S.; Otero, A.; Sánchez-Prada, J.; Villaseñor, E. *J. Organomet. Chem.*, in press.

(20) Tebbe, F. N.; Parshall, G. W. *J. Am. Chem. Soc.* **1971**, *93*, 3793.

(21) (a) Antiñolo, A.; Fajardo, M.; Jalón, F.; López-Mardomingo, C.; Otero, A.; Sanz-Bernabé, C. *J. Organomet. Chem.* **1989**, *369*, 187. (b) Antiñolo, A.; Camanyes, S.; Carrillo-Hermosilla, F.; Fajardo, M.; García-Yuste, S.; Lledós, A.; Lluch, J. M.; Maseras, F.; Moreno, M.; Otero, A. *J. Am. Chem. Soc.* **1997**, *119*, 6107. (c) Antiñolo, A.; Carrillo-Hermosilla, F.; García-Yuste, S.; Lanfranchi, M.; Otero, A.; Pellinghelli, M. A.; Prashar, S.; Villaseñor, E. *Organometallics* **1996**, *15*, 5507.

Scheme 2



2.2.1. $\text{Cp}'_2\text{Nb}(\eta^2\text{-H}_2\text{B}(\text{O}_2\text{C}_6\text{H}_4))$ (1). The ^1H NMR spectrum (C_6D_6 , 300 MHz) of complex **1** shows a broad high-field peak appearing at δ -9.54 , which is integrated for a total of two hydrogens and has been assigned to the two hydride ligands. The fact that a single signal is observed for the two hydrides denotes that they are equivalent. Moreover, an AA'BB' spin system for the four protons in the Cp' rings was observed and two signals integrated for four protons each were found. These data are also consistent with a symmetrical disposition of the two hydrides around the niobium atom. The disposition of the Cp' rings around the niobium atom was further corroborated by ^{13}C NMR spectroscopic studies, in which three resonances appear that correspond to the nonequivalent carbon atoms in the cyclopentadienyl groups. Variable-temperature ^1H NMR studies reveal that the signals in all the studied range of temperatures remain unmodified and therefore that the symmetrical disposition of the hydrides remains unchanged. In addition, complex **1** shows, in the ^{11}B NMR spectrum, a broad signal at δ 54.5 that is situated downfield from that found for the hydridoborate compound $\text{Cp}_2\text{Nb}(\eta^2\text{-H}_2\text{BH}_2)^9$ (δ 40.5) but has a chemical shift similar to that found in the related complex $\text{Cp}^*_2\text{Nb}(\eta^2\text{-H}_2\text{B}(\text{O}_2\text{C}_6\text{H}_3\text{-3-}^t\text{Bu}))$ (δ 60.9), which has been characterized as a hydridoborate compound.¹³ However, $\text{Cp}^*\text{Ta}(\text{H})_2(\text{B}(\text{O}_2\text{C}_6\text{H}_4))$ ($\text{Cp}^* = \text{C}_5\text{Me}_5$),¹³ which was proposed as a typical d^0 boryl species, shows a downfield chemical shift resonance (δ 73.5).

In summary, from an experimental point of view there is evidence that complex **1** should have a symmetrical structure for the two hydrides in a $\eta^2\text{-H}_2\text{BR}_2$ -containing niobocene complex (see Scheme 1). However, we cannot rule out some contribution of boryl character to this complex.

Complexes **2** and **3**, however, show some kind of dynamic behavior in solution because coalescence processes were observed in the variable-temperature ^1H NMR spectroscopic studies, although these processes were different for both complexes. These processes will be discussed further in the next section.

2.2.2. $\text{Cp}'_2\text{Nb}(\eta^2\text{-H}_2\text{B}(\text{C}_8\text{H}_{14}))$ (2). Surprisingly, complex **2** displays an unusual ^1H NMR spectrum (toluene-

d_8 , 300 MHz), in that an odd temperature dependence for their ^1H NMR spectra was observed. For instance, at low temperature (203 K) four peaks are observed integrated for a total of eight protons, which correspond to the hydrogen atoms of the Cp' rings. Such a set of signals may indicate an asymmetrical disposition of the two hydrides around the niobium atom. When the temperature is increased, coalescence processes take place and the spectrum changes from having four peaks to having two peaks. Each signal in the latter spectrum is integrated for four protons. In fact, two coalescence processes were observed: at 233 K the two most downfield signals of the Cp' protons coalesce, and this process takes place with a ΔG^\ddagger value of 22.8 kcal/mol. Subsequently, at 243 K the other two peaks coalesce to give the characteristic spectrum at high temperature. In this second process, the ΔG^\ddagger value measured was 23.8 kcal/mol. The difference in temperature of these two coalescence processes is due to the separation between the decoalesced signals. The difference in ΔG^\ddagger values falls into acceptable limits of experimental error for this kind of measurement. In addition, a single resonance for the two equivalent hydrides, appearing at δ -15.20 , was observed in the variable-temperature ^1H NMR spectra. The resonance appears as a sharp peak at low temperatures and as a broad peak, with widths as high as 300 Hz, at high temperatures. The existence of four peaks for the Cp' protons in the ^1H NMR spectrum at low temperature (203 K) indicates that they have chemically different environments, although this situation changed when the temperature was raised. However, the two hydrogen ligands exhibit just a single resonance (more or less broadened) in all the ranges of temperatures. In addition, complex **2** shows a resonance in the ^{11}B NMR spectrum at δ 57.60 , similar to that found for complex **1**.

Different structural situations can be proposed to explain the dynamic behavior. One possibility is the interconversion between a symmetrical $\text{Nb}-\eta^2\text{-H}_2\text{BR}_2$ borate or $\text{Nb}(\text{H})_2\text{BR}_2$ boryl and an asymmetrical $\text{Nb}(\text{H})-\eta^2\text{-(H-B)}\text{R}_2$ borane structure via an interchange between the two hydrogens and the boron atom. An alternative could be the hindered rotation of the Cp' ring in a symmetrical $\text{Nb}-\eta^2\text{-H}_2\text{BR}_2$ structure. In the complex $\text{Cp}_2\text{Nb}(\eta^2\text{-H}_2\text{B}(\text{C}_8\text{H}_{14}))$ ¹² nondynamic behavior was observed and a single signal for both hydrides was found in the ^1H NMR spectra. This complex was described¹² as the *endo*-hydridoborate isomer.²² The proposed structure was corroborated by means of an X-ray diffraction study. Conversely, in another related tantalocene complex, synthesized by the reaction with *B*-chloro-5-methylcatecholborane,^{11a} it was observed that the *exo* isomer of the boryl-dihydride species displayed in its ^1H NMR spectra a broadening of the signal corresponding to the protons of the Cp ring upon decreasing the temperature. This phenomenon suggested the onset of decoalescence, but this situation was not achieved even though the ^1H NMR spectrum was studied at temperatures as low as -80 °C. The authors imply the existence of a fluxional process to be responsible for this decoalescence.^{11a}

(22) The *endo*/*exo* designation refers to the stereochemical orientation of BR_2 within the metallocene wedge.

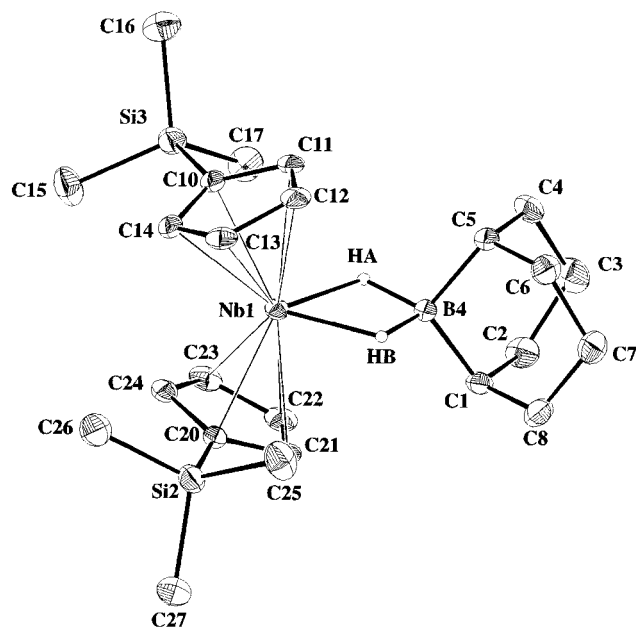


Figure 1. X-ray structure of Nb(η^5 -C₅H₄SiMe₃)₂(η^2 -H₂BC₈H₁₄) (**2**).

Table 1. Selected Bond Lengths (Å) and Angles (deg) for **2**

Nb(1)–C(Cp) (mean)	2.364(4)	Nb(1)–HB	1.85(3)
Nb(1)–B(4)	2.419(5)	B(4)–HA	1.38(4)
Nb(1)–HA	1.82(4)	B(4)–HB	1.28(3)
HA–Nb(1)–HB	66.0(15)	C(5)–B(4)–C(1)	107.1(4)
HA–B(4)–HB	97(2)	C(5)–B(4)–Nb(1)	127.1(3)
Nb(1)–HA–B(4)	97.2(12)	C(1)–B(4)–Nb(1)	125.8(3)
Nb(1)–HB–B(4)	99.6(10)		

X-ray Diffraction Study of Cp'₂Nb(η^2 -H₂B(C₈H₁₄)) (2**).** Crystals of **2** suitable for X-ray diffraction were obtained by crystallization from hexane. The single-crystal X-ray structure of **2** is shown in Figure 1. Selected bond distances and bond angles are listed in Table 1. A more complete listing of distances and angles, as well as the atomic coordinates, can be found in the Supporting Information.

Complex **2** crystallizes in the monoclinic space group *P*₂₁/*n* with one molecule in the asymmetric unit cell. The local coordination geometry around the Nb atom can be described as a pseudo-tetrahedral complex with two cyclopentadienyl rings bonded to the metal in a η^5 mode and two hydrides comprising the immediate coordination sphere. The distances between the metal atom and the centroids of the Cp rings are 2.0386(6) and 2.0379(5) Å, and the angle Cent(1)–Nb(1)–Cent(2) is 140.48(2)° (Cent(1) is the centroid of C(10)–C(14), and Cent(2) is the centroid of C(20)–C(24)). This value agrees with a Nb(III) formulation. The orientation of the Cp rings is eclipsed, as indicated by the value of the torsion angle being near 1°.

Despite their proximity to heavy niobium nuclei, the bridging hydride positions could be located in difference Fourier maps and their positional parameters were refined isotropically. It is noteworthy that these hydrides are symmetrically disposed within the bridging Nb–H–B linkages. The Nb(1)–B(4) distance is 2.419(5) Å, and Nb(1)–HA and Nb(1)–HB are 1.82(4) and 1.85(3) Å, respectively. The HA–B(4) and HB–B(4) distances are 1.38(4) and 1.28(3) Å, respectively. These values are

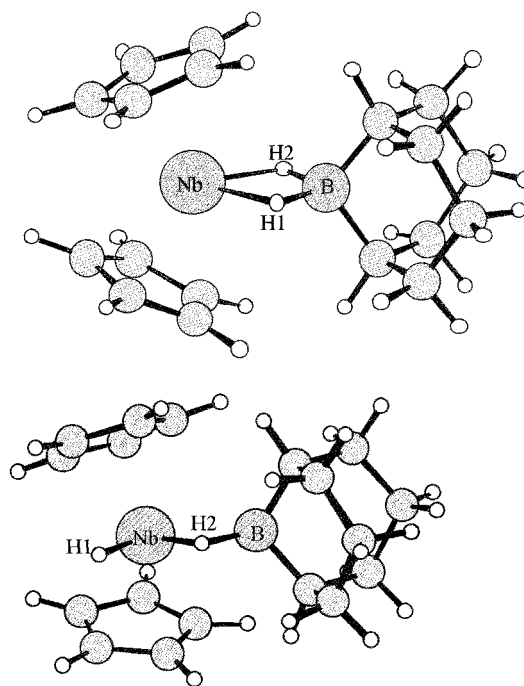


Figure 2. Optimized Becke3LYP geometries of (a, top) *endo*-Cp₂Nb(η^2 -H₂B(C₈H₁₄)) and (b, bottom) *exo*-Cp₂NbH(η^2 -HB(C₈H₁₄)).

very similar to those found in the X-ray structure of Cp₂Nb(η^2 -H₂B(C₈H₁₄)).¹² The Nb–B distances in *endo*-Cp₂Nb(H)₂(B(O₂C₆H₄))¹² and Cp₂NbH(B(O₂C₆H₄))₂,¹¹ which have been described as boryl-containing species, are significantly shorter (2.29 Å).

Theoretical Study of Cp'₂Nb(η^2 -H₂B(C₈H₁₄)) (**2**).

A great deal of information can be gained by a theoretical study of this system. Hence, theoretical work was carried out in order to localize several interesting points in the potential energy hypersurface of this system and to analyze the corresponding dynamics. However, the complete system is far too complicated for complete geometry optimizations to be affordable. Consequently, purely quantum calculations were performed on a simplified system in which the (trimethylsilyl)cyclopentadienyl groups were represented as "simple" cyclopentadienyl groups. Even with this modification the system, treated quantum chemically, has no less than 46 atoms and 256 basis functions. It is therefore clear that quantum calculations, even with the simplified system, are still quite sizable.

The quantum study of this system initially involved looking for different minima corresponding to stable structures. Both the *endo* and *exo* orientations of B(C₈H₁₄) were considered as starting points in the optimizations. Two different isomers were found. The first structure corresponds to a *endo*-(η^2 -H₂BR₂) isomer that matches the structure experimentally characterized by X-ray diffraction and described in the previous subsection of this paper. In this system both hydrides are symmetrically bound to the niobium atom (and also to the boron atom). All the attempts to find an asymmetrical *endo* structure ended at the same *endo* symmetrical structure. The second structure, on the other hand, corresponds to an *exo*-(η^2 -(H–B)R₂) borane isomer in which only one hydride is shared between the boron and the niobium atoms. Parts a and b of Figure 2 depict

Table 2. Relevant B3LYP Optimized Parameters (Distances in Å and Angles in deg) for the *endo*-(η^2 -H₂BR₂) and *exo*-(η^2 -HB)R₂ Isomers of Cp₂Nb(H₂B(C₈H₁₄))

	<i>endo</i> -(η^2 -H ₂ BR ₂)	<i>exo</i> -(η^2 -HB)R ₂
Nb–H ₁	1.900	1.744
Nb–H ₂	1.900	1.861
Nb–B	2.418	2.371
B–H ₁	1.342	3.281
B–H ₂	1.342	1.338
Nb–C(Cp) ^a	2.448	2.466
H ₁ –Nb–H ₂	67.1	70.5
Nb–H ₁ –B	94.9	44.3
Nb–H ₂ –B	94.9	94.2
H ₁ –B–H ₂	103.0	70.5

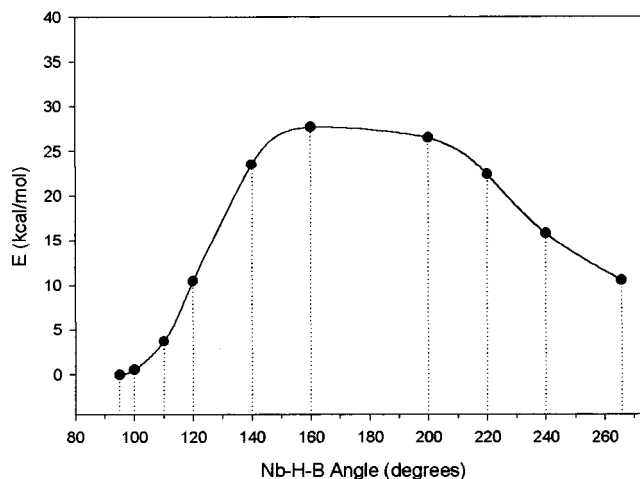
^a Mean values.

the structures found, and Table 2 displays relevant geometrical structural information corresponding to both isomers.

Although the two regioisomers (*exo* and *endo*) had been synthesized and structurally characterized for Cp₂TaH₂(B(O₂C₆H₄)),^{11a} only the *endo* isomers have been characterized for the niobium analogues.^{12,13} However, very recently the structure *exo*-Cp₂NbH(η^2 -HB(O₂C₆H₄)) was assigned to an intermediate found in the reaction of Cp₂NbH(CH₂=CHMe) with HB(O₂-C₆H₄).^{11b} Our finding of a *exo*-(η^2 -(H–B)R₂) minimum in the potential energy surface of Cp₂NbH₂B(C₈H₁₄) supports this assignment. In agreement with experimental results presented in this paper, the most stable isomer found theoretically is the symmetrical *endo*-borate species, which in the simplified system belongs to the C_{2v} symmetry point group. The less stable asymmetrical hydridoborane isomer, a C_s structure in the simplified calculations, lies 10.5 kcal/mol above the former. In a comparison of the structural data obtained theoretically (Table 2) with those from the X-ray diffraction study (Table 1), it can be seen that there is very good agreement and so the theoretical description of the system seems to be sufficiently accurate.

Additionally, given that two different minima were found, the dynamics of the isomerization was studied. This study was performed by obtaining the potential energy profile of the reaction coordinate that leads from one minimum to the other. We took as a reaction coordinate the Nb–H–B angle, which varies from 94.9° in the *endo*-(η^2 -H₂BR₂) borate isomer to 265.8° in the *exo*-(η^2 -H–B)R₂ borane. The procedure consisted of fixing the Nb–H–B angle at different values starting from the borate-containing minimum and going to the *exo*-borane-containing one, followed by optimization of the whole structure barring this angular parameter. The resulting potential energy profile is depicted in Figure 3. The potential energy barrier to the isomerization process can be estimated as approximately 28 kcal/mol, as ascertained from Figure 3.

Upon reaching this point, it is necessary to find an explanation for the spectroscopic ¹H NMR data described in the preceding subsection. The isomerization from the most stable symmetrical *endo*-borate to the *exo*-borane cannot be the observed process. As explained above, we detected a dynamic process with a free energy barrier of ca. 23 kcal/mol. At the low-temperature end, the four protons directly bound to the carbon atoms in the Cp' groups produce a total of four different signals,

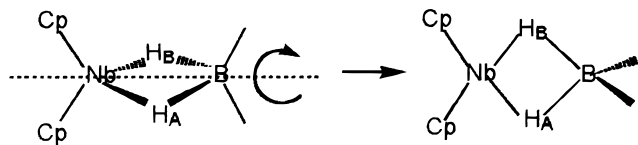
**Figure 3.** Potential energy profile for the *endo*-(η^2 -H₂BR₂) borate \rightarrow *exo*-(η^2 -H–B)R₂ borane isomerization in Cp₂NbH₂-(B(C₈H₁₄)).

which overall are integrated as two protons each, due to the fact that each has a different chemical environment. This would be the case if the Cp' groups did not have essentially free rotation. We will return later to this question.

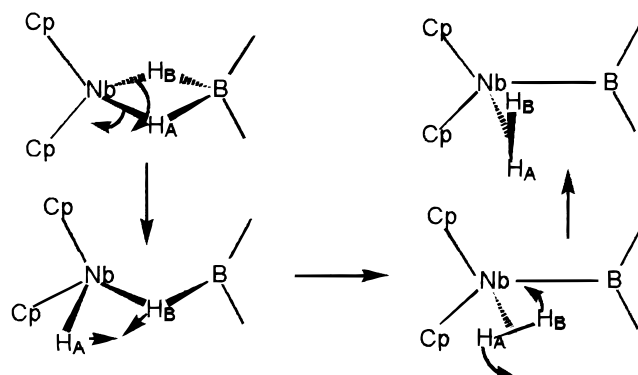
Although there is not experimental evidence for hydride exchange in compound **2**, since the hydride ligands are related by a C₂ axis, theoretical calculations were performed, aimed at studying further the dynamics and structure of complex **2**. In particular, we studied the dynamics of the exchange process of both equivalent hydrides in *endo*-Cp₂Nb(η^2 -H₂B(C₈H₁₄)) by determining the potential energy barrier of such a process. There are several options available when devising a mechanism for the exchange of these hydrides. One possibility (mechanism A, Scheme 3) implies the rotation of the η^2 -(H₂BBN) (BBN = 9-borabicyclononane) fragment around the imaginary axis that passes through the niobium and the boron atoms (this axis is a real symmetry axis in the C₂ minimum found previously). We have also considered another possibility (mechanism B, Scheme 3), which consists of a reaction path that passes through the *exo*-hydridoborane intermediate. With the most stable minimum energy borate-containing structure found as a starting point, the geometrical deformation consisting of the opening of an Nb–H–B angle, discussed above, leads to the borane isomer. Next, both hydrides approach each other in such a way that a dihydrogen ligand is formed. Finally, this dihydrogen ligand rotates by 180° and the process goes back to its origins, the hydrides having been exchanged. Although this mechanism seems very speculative, the pairwise hydrogen exchange via an η^2 -H₂ species is a well-known process in transition-metal polyhydrides.²³ A schematic representation of both mechanisms is depicted in Scheme 3.

(23) Maseras, F.; Lledós, A.; Clot, E.; Eisenstein, O. *Chem. Rev.* **2000**, *100*, 601

Scheme 3
MECHANISM A



MECHANISM B



The potential energy through exchange mechanism A amounts to 37.3 kcal/mol with respect to the absolute minimum for this complex. As for exchange mechanism B, some adjustments need to be made. For instance, no minimum corresponding to a true dihydrogen complex could be located; therefore, the energy of a tentative dihydrogen complex was calculated by forcing the H–H distance to be 0.80 Å, a representative value of the H–H distance in dihydrogen complexes. By doing this, a “transition state structure” corresponding to the rotation of this dihydrogen ligand could be located, and this structure would correspond to the highest energy point in the exchange process through mechanism B. The corresponding value for the potential energy barrier is 47.5 kcal/mol, which is much higher than that of mechanism A. In summary, it seems clear that the exchange process of the two hydrides in this complex is an energy costly process that only will be operative at high temperatures. It would take place through a mechanism similar to mechanism A.

We now turn our attention to the dynamic process with a ΔG^\ddagger value of ca. 23 kcal/mol and attempt to put forward a plausible explanation for it. There are dozens of organometallic complexes that have two cyclopentadienyl groups (or related groups) around a metal atom. In general, it is widely accepted that the rotational motion of such ligands takes place with almost no energy barrier, so that the cyclopentadienyl group rotates freely at all but the lowest of temperatures. This being the case, it is clear that one should expect only two different NMR signals for the protons in the monosubstituted Cp groups, because their rapid rotation averages the different chemical environments of the protons in the ring, with the exception of those coming specifically from the ring itself. This means that at the low-temperature end, in which four NMR signals were observed experimentally rather than two, it could be the case that the rotation of the Cp' group stops.²⁴ In fact,

the Cp' groups present in this complex include a quite voluminous group, Si(CH₃)₃, which could give rise to steric interactions on rotation due to collision with the C–H bond perpendicular to the NbH₂B plane in the BBN group. The following discussion deals with the determination of the energy barrier for this process.

To determine the potential energy barrier for the process of rotation of the Cp' groups, it is necessary to take into account their structure in an explicit way. The minimum energy structure should be recalculated with trimethylsilyl groups included, and the transition state structure for the rotation of one Cp' group should also be located. While the minimum energy structure will still belong to the C₂ symmetry point group, the transition state structure will certainly not and will be C₁. This fact alone makes the calculation extremely difficult due to the significant increase in basis functions and electrons and the lack of symmetry. However, given that we are interested in studying the steric hindrance to the rotation process, we carried out these calculations using a hybrid QM/MM method, IMOMM, in which we treated the complex quantum chemically (Becke3LYP) and included a molecular mechanics (MM3) description of the two Si(CH₃)₃ groups. This approximate description will be quite accurate if only steric interactions are important,²⁵ which seems to be the case here.

To determine the potential energy barrier associated with the rotation of the Cp' rings, the minimum energy structure was recalculated for the real complex, optimizing its geometry with the IMOMM(Becke3LYP:MM3) method (Figure 4a). According to X-ray diffraction data, the complete species seems to belong to the C₂ symmetry point group, and the minimum was sought with this requirement enforced. As far as the rotational transition state is concerned, the lowest energy structure was calculated in which one of the Cp' rings projects its Si(CH₃)₃ group toward the BR₂ part of the borate ligand (Figure 4b). This means that we can, at best, estimate the barrier height because the transition state was not precisely located. In addition, we explored the possibility of both Cp' groups rotating synchronously, but the resulting energy barrier is much higher than in the previous case.

Table 3 shows some geometrical parameters resulting from the IMOMM(Becke3LYP:MM3) calculations, and Figure 4 displays the structures found. The IMOMM calculations reveal that the structure found for the potential energy minimum differs little geometrically from that found with the pure quantum-mechanical model, at least with respect to the environment of the metal atom and the hydrides. This can be seen clearly by comparing the data in Tables 2 and 3. However, the study of the rotation of one of the Cp' groups reveals severe steric hindrance in the region in which the Si(CH₃)₃ group passes over the C–H bond in the BBN fragment, with the Cp' ring becoming more inclined to make room for this contact. According to this, the mean value of the C(Cp)–Nb distances increases from 2.459 Å in the minimum to 2.530 Å in the rotational transition state and the Nb–H distances are also lengthened. In fact, even with the Cp ring moving away, the closest

(24) Long, N. J. *Metalloenes, An Introduction to Sandwich Complexes*; Blackwell Science: Oxford, U.K., 1998; p 165.

(25) Maseras, F. *Top. Organomet. Chem.* **1999**, *4*, 165.

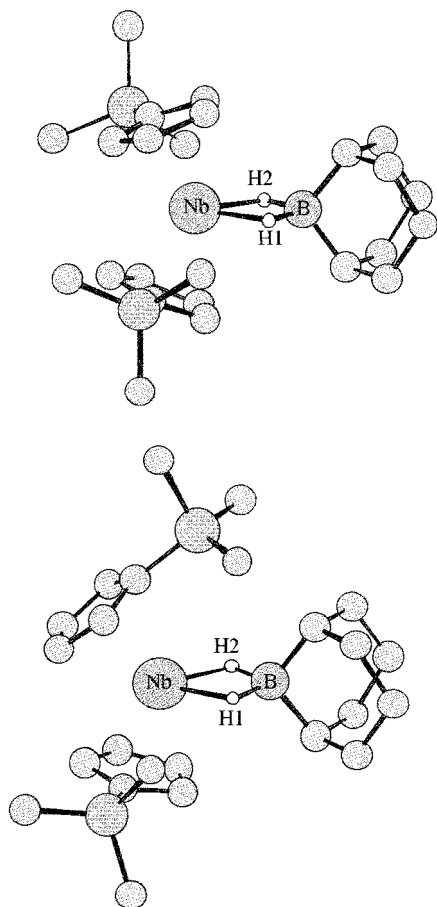


Figure 4. IMOMM (Becke3LYP:MM3) optimized geometries of (a, top) $\text{Nb}(\eta^5\text{-C}_5\text{H}_4\text{SiMe}_3)_2(\eta^2\text{-H}_2\text{BC}_8\text{H}_{14})$ and (b, bottom) the transition state for the rotation of a Cp' ring.

Table 3. Selected IMOMM (B3LYP:MM3) Optimized Parameters (Distances in Å and Angles in deg) for the Minimum and Rotational Transition State of the $\text{Nb}(\eta^5\text{-C}_5\text{H}_4\text{SiMe}_3)_2(\eta^2\text{-H}_2\text{B}(\text{C}_8\text{H}_{14}))$ Complex

	minimum	rotational transition state
Nb–H ₁	1.897	1.925
Nb–H ₂	1.897	1.939
Nb–B	2.413	2.482
B–H ₁	1.347	1.341
B–H ₂	1.347	1.346
Nb–C(Cp) ^a	2.459	2.530 ^b
Nb–C(Cp) ^a	2.459	2.474 ^c
H ₁ –Nb–H ₂	67.5	65.0
Nb–H ₁ –B	94.6	97.3
Nb–H ₂ –B	94.6	96.5
H ₁ –B–H ₂	103.2	101.2

^a Mean values. ^b Rotating ring. ^c Nonrotating ring.

contact between the H atom in the borate ligand and one of the H atoms in the trimethylsilyl groups is 2.341 Å. The transition state structure was not precisely located but was estimated. In this way, the potential energy barrier found amounts to 21.0 kcal/mol, in excellent agreement with the experimental value of ca. 23 kcal/mol. This confirms that the dynamic process responsible for the coalescence of the NMR signals is, in fact, the rotation of the cyclopentadienyl groups.

There is, however, another peculiarity in the ¹H NMR spectrum that remains unexplained, i.e., the temperature-dependent width of the peak corresponding to the

two hydride ligands. When studying the isomerization process that interconverts the borate-containing and borane-containing structures, we found that the potential energy profile was quite damped in the neighboring areas of the minimum near the borate-containing structure. This can be seen in Figure 3, where it is easy to quantify an energy increase of only 3.7 kcal/mol on opening the Nb–H–B angle from 95 to 110°. In this way, upon increasing the temperature, the vibrational motion of the system along this potential energy profile would be somewhat loose. This means that the hydrides can be found in a rather wide area of the potential energy surface, causing the broadening of the NMR signals corresponding to these protons, as was experimentally detected. On the other hand, it is also possible that the unusual width is the result of the coupling of both hydride atoms to the ¹¹B atom.

2.2.3. $\text{Cp}'_2\text{Nb}(\eta^2\text{-H}_2\text{BH}_2)$ (3). The ¹H NMR spectrum of complex **3** shows a sharp singlet signal at δ –0.04 and two pseudotriplet resonances at δ 4.08 and 5.41, corresponding to the (trimethylsilyl)cyclopentadienyl ligands in a symmetrically bent niobocene disposition. In addition, a very broad peak, centered at δ –16.37, was found, and this corresponds to the bridged hydrogen atoms of the $\eta^2\text{-BH}_4$ ligand. The peak corresponding to the terminal boron hydride atoms could not be observed, due to the fact that it was obscured by the peak at δ 5.41 from the cyclopentadienyl ring protons. The resonance in the ¹¹B NMR spectrum at δ 40.0 ppm is consistent with a hydridoborate character.¹⁸ The IR spectrum of complex **3** shows two bands in the terminal B–H region at 2466 and 2424 cm^{-1} and two bands in the bridging M–H–B region at 1750 and 1739 cm^{-1} .

As for complex **2**, a variable-temperature ¹H NMR study was also performed for **3**. At temperatures below 250 K a resonance at δ 5.60 was observed, corresponding to the terminal hydrogen atoms of the BH_4 ligand. However, upon increasing the temperature above 250 K, the resonances at δ –16.50 and 5.60 broaden and shift toward each other, starting a coalescence process. Coalescence of these signals was observed at 348 K, and the ΔG^\ddagger value for this process was determined to be 13.6 kcal/mol. It seems clear that the dynamic process behind this coalescence is exchange of the bridging (b) and terminal hydrides (t) in the $\eta^2\text{-BH}_4$ group. The value found for the free energy barrier is similar to those found for the exchange processes in related complexes, namely $\text{Cp}_2\text{Nb}(\eta^2\text{-BH}_4)$ ($\Delta G^\ddagger = 14.6$ kcal/mol), $\text{Cp}'_2\text{Nb}(\eta^2\text{-BH}_4)$ ($\Delta G^\ddagger = 16.4$ kcal/mol), and $\text{CpCp}^*\text{Ta}(\eta^2\text{-BH}_4)$ ($\Delta G^\ddagger = 16.4$ kcal/mol).^{9d,10} A very recent thorough study of the hydrogen scrambling processes in the tetrahydroborate derivatives of group 5 *ansa*-metallocenes has proved that the free energy barrier to bridge–terminal exchange is considerably reduced when the bridging unit imposes significant structural changes in the metallocene ($\Delta G^\ddagger = 8.3$ kcal/mol in $[\text{Nb}\{(\eta\text{-C}_5\text{H}_4)\text{CMe}_2(\eta\text{-C}_5\text{H}_4)\}(\eta^2\text{-BH}_4)]$).²⁶ To clarify the mechanism of the H_b → H_t exchange in $\text{Cp}'_2\text{Nb}(\eta^2\text{-BH}_4)$, we have carried out theoretical calculations on the model system $\text{Cp}_2\text{Nb}(\eta^2\text{-BH}_4)$, which will be presented in the next section.

(26) Conway, S. L.; Doerrer, L. H.; Green, M. L. H.; Leech, M. A. *Organometallics* **2000**, *19*, 630.

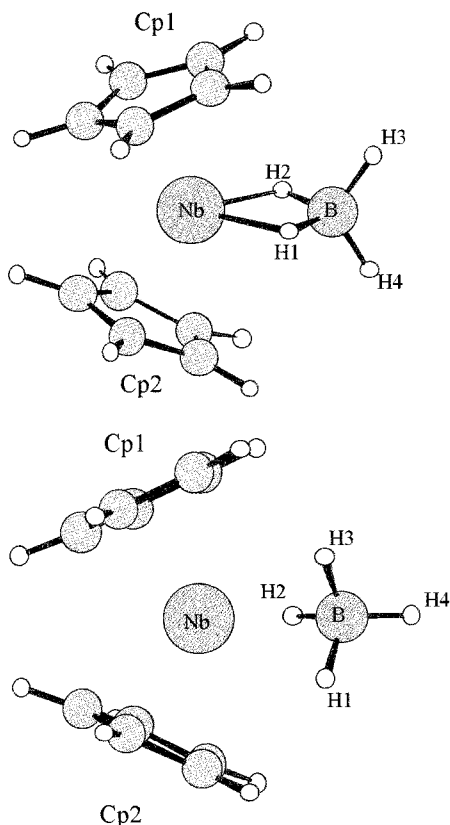


Figure 5. Optimized Becke3LYP geometry of (a, top) Cp₂Nb(η^2 -H₂BH₂) and (b, bottom) the transition state for the H_b → H_t exchange.

Table 4. Relevant B3LYP Optimized Parameters (Distances in Å) for the Minimum and the H-Bridging/H-Terminal Transition State of the Cp₂Nb(η^2 -H₂BH₄) Complex

	minimum	transition state
Nb–H ₁	1.906	2.329
Nb–H ₂	1.906	1.943
Nb–H ₃	3.165	2.333
Nb–H ₄	3.165	3.500
Nb–B	2.362	2.333
B–H ₁	1.321	1.217
B–H ₂	1.321	1.318
B–H ₃	1.200	1.217
B–H ₄	1.200	1.196
Nb–C(Cp1) ^a	2.445	2.472
Nb–C(Cp2) ^a	2.445	2.472
C–C(Cp1) ^a	1.433	1.431
C–C(Cp2) ^a	1.433	1.431
Nb–C(Cp1) ^b	2.375/2.495	2.405/2.559
Nb–C(Cp2) ^b	2.375/2.495	2.397/2.561

^a Mean values. ^b Maximum and minimum values.

Theoretical Study of Cp₂Nb(η^2 -H₂BH₂). The optimized geometry of the model complex Cp₂Nb(η^2 -H₂BH₂) is depicted in Figure 5a, and its main geometrical parameters are collected in Table 4. The calculated structure is in good agreement with the X-ray structure determination.^{9b} The molecular structure confirms the assignment of a bidentate η^2 -BH₄ binding mode. The bridging B–H_b bond lengths are longer than the terminal B–H_t bond lengths. The weakening of the bridging B–H_b bonds is also reflected in the calculated vibrational modes (ν (B–H_b), 1728 and 1719 cm⁻¹; ν (B–H_t), 2615 and 2556 cm⁻¹). These values agree reasonably well with the experimental IR vibrational data of

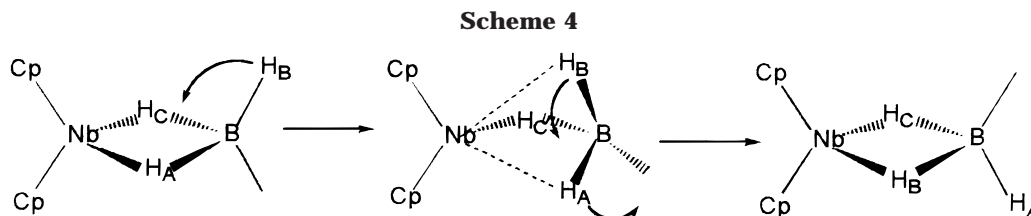
this complex.^{9c} The preference of BH₄⁻ for the η^2 coordination mode in the Cp₂Nb(BH₄) complex can be explained with the electron-counting concepts previously applied to the rationalization of the BH₄ coordination to transition-metal systems.^{1b,27} The equilibrium structure will obey the 18-electron rule.

The exchange process between terminal and bridging hydrogen atoms of a tetrahydroborate ligand coordinated in a bidentate mode is generally considered to involve a change in the coordination mode of the ligand.^{1a,10} Thus, there are in principle two possible mechanisms: via a monodentate BH₄ ligand (dissociative mechanism) and via a tridentate BH₄ ligand (associative mechanism). Green^{10,26} has proposed that in group 5 metallocene tetrahydroborate complexes the mechanism is associative and that the formation of a η^3 -BH₄ intermediate is accompanied by an $\eta^5 \rightarrow \eta^3$ ring shift of one of the cyclopentadienyl rings.

We have studied by means of DFT calculations the mechanism of the H_b/H_t exchange in Cp₂Nb(η^2 -BH₄). We started our search for the transition state of the exchange process with the optimization of two different structures containing “ideal” monodentate and tridentate BH₄ ligands, which were obtained by forcing a local C_{3v} symmetry on Nb–BH₄. Neither of these structures corresponds to a stationary point. The preference for the associative mechanism has already been put forward in these preliminary calculations. Whereas the ideal η^1 structure lies 34.3 kcal/mol above the η^2 minimum, the η^3 structure is found 18.9 kcal/mol above the minimum. We used the ideal η^3 structure as a starting point for the direct search of the transition state in the full potential energy hypersurface. This strategy has already been successfully applied to the location of transition states for tetrahydroborate H_b/H_t exchanges.²⁸ In this way we found a stationary point that was characterized as a transition state: it has a single negative eigenvalue in the calculated Hessian matrix. This transition state is shown in Figure 5b, and its main bond distances and angles are collected in the second column of Table 4. In the transition state the BH₄ unit is clearly tridentate, although the local C_{3v} symmetry on the Nb–BH₄ moiety is lost. One of the bridging H atoms is closer to the metal than the other two, and the angle Nb–B–H_t is smaller than 180°. The B–H bond distances for the two further H_b atoms are very similar to that of the B–H_t bond, indicating a weak Nb–H interaction. In going from the equilibrium structure to the transition state, changes in the metal–cyclopentadienyl distances are small (see Table 4). The angle between the Cp rings is slightly reduced to accommodate the tridentate tetrahydroborate, as can be seen by comparing the shortest and longest Nb–C(Cp) distances in both structures. This fact could explain why the ΔG^\ddagger value is sensibly reduced in *ansa*-metallocenes, in which the *ansa* bridge imposes an important reduction of the angle between the ring planes.²⁶ The C–C distances of the Cp ligand remain

(27) (a) Lledós, A.; Duran, M.; Jean, Y.; Volatron, F. *Inorg. Chem.* **1991**, *30*, 4440. (b) Volatron, F.; Duran, M.; Lledós, A.; Jean, Y. *Inorg. Chem.* **1993**, *31*, 951. (c) Jarid, A.; Lledós, A.; Jean, Y.; Volatron, F. *Inorg. Chem.* **1993**, *32*, 4695.

(28) (a) Jarid, A.; Lledós, A.; Jean, Y.; Volatron, F. *Chem. Eur. J.* **1995**, *1*, 436. (b) Demachy, I.; Esteruelas, M. A.; Jean, Y.; Lledós, A.; Maseras, A.; Oro, L. A.; Valero, C.; Volatron, F. *J. Am. Chem. Soc.* **1996**, *118*, 8388.



almost unchanged, indicating that a change in the coordination mode of the Cp ligand does not occur.

The energy of the transition state is 13.9 kcal/mol above that of the equilibrium structure. This value is in excellent accord with those experimentally determined for $\text{Cp}_2\text{Nb}(\eta^2\text{-BH}_4)$ ($\Delta G^\ddagger = 14.6$ kcal/mol)^{9d} and complex **3** ($\Delta G^\ddagger = 13.6$ kcal/mol). Analysis of the eigenvalue associated with the only imaginary frequency ($440.5i$ cm^{-1}) sheds light on the mechanism of the exchange. The transition vector has no components in the Cp rings. The reaction coordinate is essentially the rotation around one of the B–H_b bonds in the minimum (Scheme 4). The same mechanism was found for the hydrogen exchange in $[\text{Cu}(\text{PH}_3)_2(\eta^2\text{-BH}_4)]$, with an energy barrier of 11.7 kcal/mol.^{28a}

3. Concluding Remarks

New borate-containing niobocene complexes, $[\text{Nb}(\eta^5\text{-C}_5\text{H}_4\text{SiMe}_3)_2(\eta^2\text{-H}_2\text{BR}_2)]$ ($\text{R}_2 = \text{O}_2\text{C}_6\text{H}_4$ (**1**), C_8H_{14} (**2**), H_2 (**3**)), have been prepared by reaction of $[\text{Nb}(\eta^5\text{-C}_5\text{H}_4\text{-SiMe}_3)_2(\text{H})_3]$ and the appropriate boranes. The experimental conditions for the process, which probably involves the initial interaction of the trihydride niobocene with the borane, are clearly dependent on the acid character of the borane. These processes demonstrate the validity of a previous theoretical study showing that the interaction of a Lewis acid with the lateral hydride of a trihydride species stabilizes a dihydrogen and assists its elimination. NMR spectroscopic data and an X-ray crystal structure for complex **2** indicate that a η^2 -borate-containing structure must be considered for these complexes. Complex **1** exhibits a static behavior in solution, even though a dynamic behavior for **2** and **3** was found. Theoretical studies of **2** were carried out. The quantum studies established that the *endo*-(η^2 -borate) isomer is the most stable, which is in agreement with the X-ray crystal structure data obtained. An *exo*-(η^2 (H–B)borane) isomer was found about 10 kcal/mol above the most stable structure. In addition, theoretical calculations to study the dynamics of **2** were also considered. They allowed us to characterize the dynamic process responsible for the coalescence of the Cp' NMR signals as the rotation of the cyclopentadienyl groups. Finally, an exchange between the bridging and terminal hydrides in the η^2 -BH₄ group of **3** has been proposed as being responsible for the dynamic behavior observed for this compound. A theoretical study of the hydrogen exchange has shown that it takes place with an associative mechanism, via a η^3 -BH₄ transition state.

Experimental Section

General Procedures. All reactions were carried out using Schlenk techniques under an atmosphere of dry nitrogen. Solvents were distilled from appropriate drying agents and degassed before use. The complexes Cp_2NbH_3 and $\text{Cp}_2\text{Nb}(\text{H})$

(L) (L = CO, CN(2,6-Me₂C₆H₃), ^tBuOOCH=CHCOO^tBu) was prepared by literature procedures.^{18,21} Borane reagents, catecholborane, 9-borabicyclononane, and the BH₃·THF adduct, were purchased from Aldrich and used as received. ¹H and ¹³C NMR spectra were obtained on a Varian Unity 300 spectrometer. Trace amounts of protonated solvents were used as references, and chemical shifts are reported in parts per million relative to SiMe₄. ¹¹B NMR spectra were recorded on a Varian Unity 300 spectrometer operating at 96.2 MHz, and the spectra were referenced to a BF₃·Et₂O external standard solution. IR spectra were obtained in the region 200–4000 cm^{-1} using a Perkin-Elmer 883 spectrophotometer.

Nb(η^5 -C₅H₄SiMe₃)₂(η^2 -H₂BO₂C₆H₄) (1**).** Nb(η^5 -C₅H₄SiMe₃)₂(H)₃ (0.30 g, 0.80 mmol) was dissolved in 30 mL of toluene to give a light brown solution. To this solution was added 0.80 mmol of HBO₂C₆H₄, and the mixture was stirred at 40 °C for 3 h. The resulting dark brown solution was filtered, and the solvent was removed, from the filtrate, in vacuo. After the solid was washed with 10 mL of hexane, complex **1** was obtained as a brown microcrystalline solid (yield: 88%). IR (Nujol/PET, cm^{-1}): 1690 (w), 1676 (w) bridging M–H–B region, 1248 (m), 836 (s). ¹H NMR (300 MHz, C₆D₆): δ –9.54 (s, 2H, Nb–H–B), 0.06 (s, 18H, SiMe₃), 4.37 (m, 4H, C₅H₄), 5.23 (m, 4H, C₅H₄), 7.00 (m, 4H, B(O₂C₆H₄)). ¹³C{¹H} NMR (75 MHz, C₆D₆): δ 1.1 (SiMe₃), 95.2, 97.6, 92.1 (C₅H₄), 110.8, 121.2, 152.9 (B(O₂C₆H₄)). ¹¹B NMR (96.2 MHz, C₆D₆): δ 54.5. Anal. Calcd for C₂₂H₃₂BNbO₂Si₂: C, 54.09; H, 6.62. Found: C, 53.72; H, 6.49.

Nb(η^5 -C₅H₄SiMe₃)₂(η^2 -H₂BC₈H₁₄) (2**).** Complex **2** was prepared in a manner similar to that for **1**, to obtain a dark green solid (yield: 85%). IR (Nujol/PET, cm^{-1}): 1704 (w), 1695 (w) bridging M–H–B region, 1254 (m), 830 (s). ¹H NMR (300 MHz, C₆D₆): δ –15.20 (br s, 2H, Nb–H–B), –0.03 (s, 18H, SiMe₃), 1.50 (m, 14H, BC₈H₁₄), 4.00 (br s, 4H, C₅H₄), 5.54 (br s, 4H, C₅H₄). ¹³C{¹H} NMR (75 MHz, C₆D₆): δ 1.2 (SiMe₃), 24.5, 34.0 (BC₈H₁₄), 98.0, 103.0 (br peaks, C₅H₄, the peak corresponding to C1 carbon atoms was probably overlapped). ¹¹B NMR (96.2 MHz, C₆D₆): δ 57.6. Anal. Calcd for C₂₄H₄₂BNbSi₂: C, 58.76; H, 8.65. Found: C, 58.27; H, 8.55.

Nb(η^5 -C₅H₄SiMe₃)₂(η^2 -H₂BH₂) (3**).** Nb(η^5 -C₅H₄SiMe₃)₂(H)₃ (0.30 g, 0.80 mmol) was dissolved in 40 mL of THF to give a light brown solution. This solution was cooled to –78 °C and 80 μ L (0.80 mmol) of a 1 M solution of BH₃·THF in THF was added. The mixture was stirred for 30 min. The resulting light brown solution was filtered, and the solvent was removed, from the filtrate, in vacuo. After the solid was washed with 10 mL of hexane, complex **3** was obtained as a green microcrystalline solid (yield: 90%). Alternatively, this compound can be prepared by reaction between BH₃·THF and Nb(η^5 -C₅H₄SiMe₃)₂(H)(L) (L = CO, CN(2,6-Me₂C₆H₃)) in a way similar to that described for Nb(η^5 -C₅H₄SiMe₃)₂(H)₃. When the complex Nb(η^5 -C₅H₄SiMe₃)₂(H)(^tBuOOCH=CHCOO^tBu) was used, the solution was heated at 40 °C for 2 h, to obtain the complex **3**. IR (Nujol/PET, cm^{-1}): 2466 (s), 2424 (s) terminal B–H region, 1750 (w), 1739 (w) bridging M–H–B region, 1247 (m), 840 (s). ¹H NMR (300 MHz, C₆D₆): δ –16.37 (s, 2H, Nb–H–B), –0.04 (s, 18H, SiMe₃), 4.08 (m, 4H, C₅H₄), 5.60 (s, 2H, BH₂, measured below 250 K, see the text), 5.41 (m, 4H, C₅H₄). ¹³C{¹H} NMR (75 MHz, C₆D₆): δ 0.7 (SiMe₃), 87.0, 98.7, 103.0 (C₅H₄). ¹¹B NMR (96.2 MHz, C₆D₆): δ 40.0. Anal. Calcd. for C₁₆H₃₀BNbSi₂: C, 54.28; H, 8.48. Found: C, 54.12; H, 8.52.

Structure Determination of Complex 2. A green crystal of approximate dimensions 0.3 × 0.2 × 0.2 mm was mounted in a glass capillary. Intensity data were collected on a Nonius-MACH3 diffractometer equipped with graphite-monochromated Mo K α radiation (λ = 0.710 70 Å) using an $\omega/2\theta$ scan technique to a maximum value of 56°. Crystal are monoclinic, space group $P2_1/n$, with the following cell parameters: a = 7.714(2) Å, b = 21.9380(10) Å, c = 16.070(3) Å, β = 100.80(2)°, V = 2671.4(9) Å³, Z = 4, calculated density 1.22 g cm⁻³. Data were corrected in the usual fashion for Lorentz and polarization effects, and empirical absorption correction was based on a ψ scan²⁹ (maximum and minimum values of the transmission factor were 0.544–1.000). The structure was solved using direct methods (SIR92).³⁰ Refinement on F^2 was carried out by full-matrix least-squares techniques (SHELXL97).³¹ All non-hydrogen atoms were refined with anisotropic thermal parameters. The hydrogen atoms were included in calculated positions, except HA and HB, which were located in the difference Fourier map and were refined isotropically. Refinement (6439 reflections, 261 parameters) converged to give the following values: $R1$ = 0.0378, $wR2$ = 0.0703, GOF = 0.965 for 3495 reflections with $I > 2\sigma(I)$; $R1$ = 0.0949, $wR2$ = 0.1178 for all data. Maximum and minimum residual electron densities were 0.626 and -0.508 e Å⁻³.

Computational Details. DFT calculations on model complexes Cp₂Nb(H₂B(C₈H₁₄)) and Cp₂Nb(BH₄) were carried out with the Gaussian 98³² series of programs using the Becke3LYP functional.³³ A quasi-relativistic effective core potential operator was used to represent the 28 innermost electrons of the niobium atom.³⁴ The basis set for the niobium atom was that

associated with the pseudopotential with a standard valence double- ζ LANL2DZ contraction.³² The 6-31G(d,p) basis set was used for the boron atom and all the hydrogen atoms, except those of the Cp ligands. For the Cp and BNN hydrogen atoms, as well as for the carbon and nitrogen atoms, the 6-31G basis set was used.³⁵ Calculations on the real complex Nb(η^5 -C₅H₄-SiMe₃)₂(η^2 -H₂BC₈H₁₄) were performed using the IMOMM method,³⁶ with a program built from modified versions of two standard programs: Gaussian 92/DFT³⁷ for the quantum mechanics part and mm3 (92)³⁸ for the molecular mechanics part. The QM part of the calculations was done at the Becke3LYP level³³ using the same basis sets^{32,34,35} as for the model complexes. The MM part of the calculations used the mm3 (92) force field.³⁹ van der Waals parameters for the niobium atom were taken from the UFF force field.⁴⁰ Torsional contributions involving dihedral angles with the metal atom in the terminal position were set to zero. All geometrical parameters were optimized, except the bond distances between the QM and the MM regions of the molecule. The frozen values were 1.10 Å (C–H) in the QM part and 1.85 Å (C–Si) in the MM part.

Acknowledgment. Financial support from the Spanish Comisión Interministerial de Ciencia y Tecnología (Projects PB98-0915, PB98-0916-CO2-01, and PB-95-0023-CO1-CO2) is acknowledged. We thank Dr. F. Maseras (UAB) for invaluable technical advice on IMOMM calculations. The use of computational facilities at the Centre de Supercomputació i Comunicacions de Catalunya (C⁴) is also greatly appreciated.

Supporting Information Available: Crystal structure data for **2**, including tables of atomic positional parameters, anisotropic thermal parameters, all bond distances and angles, and hydrogen atomic coordinates. This material is available free of charge via the Internet at <http://pubs.acs.org>.

OM000221D

(29) North, A. C. T.; Phillips, D. C.; Mathews, F. S. *Acta Crystallogr.* **1968**, *A24*, 351.

(30) Altomare, A.; Cascarano, G.; Giacovazzo, C.; Guagliardi, A.; Burla, M. C.; Polidori, G.; Camalli, M. *J. Appl. Crystallogr.* **1994**, *435*–436.

(31) Sheldrick, G. M. Program for the Refinement of Crystal Structures from Diffraction Data; University of Göttingen, Göttingen, Germany, 1997.

(32) Frisch, M. J.; Trucks, G. W.; Schlegel, H. B.; Scuseria, G. E.; Robb, M. A.; Cheeseman, J. R.; Zakrzewski, V. G.; Montgomery, J. A.; Stratmann, R. E.; Burant, J. C.; Dapprich, S.; Millam, J. M.; Daniels, A. D.; Kudin, K. N.; Strain, M. C.; Farkas, O.; Tomasi, J.; Barone, V.; Cossi, M.; Cammi, R.; Mennucci, B.; Pomelli, C.; Adamo, C.; Clifford, S.; Ochterski, J.; Petersson, G. A.; Ayala, P. Y.; Cui, Q.; Morokuma, K.; Malick, D. K.; Rabuck, A. D.; Raghavachari, K.; Foresman, J. B.; Cioslowski, J.; Ortiz, J. V.; Stefanov, B. B.; Liu, G.; Liashenko, A.; Piskorz, P.; Komaromi, I.; Gomperts, R.; Martin, R. L.; Fox, D. J.; Keith, T.; Al-Laham, M. A.; Peng, A.; Nanayakkara, A.; Gonzalez, C.; Challacombe, M.; Gill, P. M. W.; Johnson, B. G.; Chen, M. W.; Wong, M. W.; Andrés, J. L.; Head-Gordon, M.; Replogle, E. S.; Pople, J. A. Gaussian 98; Gaussian, Inc., Pittsburgh, PA, 1998.

(33) (a) Lee, C.; Yang, W.; Parr, R. G. *Phys. Rev. B* **1988**, *37*, 785. (b) Becke, A. D. *J. Chem. Phys.* **1993**, *98*, 5648. (c) Stephens, P. J.; Devlin, F. J.; Chabalowski, C. F.; Frisch, M. J. *J. Phys. Chem.* **1994**, *98*, 11623.

(34) Hay, P. J.; Wadt, W. R. *J. Chem. Phys.* **1985**, *82*, 299.

(35) (a) Hehre, W. J.; Ditchfield, R.; Pople, J. A. *J. Chem. Phys.* **1972**, *56*, 2257. (b) Hariharan, P. C.; Pople, J. A. *Theor. Chim. Acta* **1973**, *28*, 213. (c) Francl, M. M.; Pietro, W. J.; Hehre, W. J.; Binkley, J. S.; Gordon, M. S.; Defrees, D. J.; Pople, J. A. *J. Chem. Phys.* **1982**, *77*, 3654.

(36) Maseras, F.; Morokuma, K. *J. Comput. Chem.* **1995**, *16*, 1170.

(37) Frisch, M. J.; Trucks, G. W.; Schlegel, H. B.; Gill, P. M. W.; Johnson, B. G.; Wong, M. W.; Foresman, J. B.; Robb, M. A.; Head-Gordon, M.; Replogle, E. S.; Gomperts, R.; Andrés, J. L.; Raghavachari, K.; Binkley, J. S.; Gonzalez, C.; Martin, R. L.; Fox, D. J.; Defrees, D. J.; Baker, J.; Stewart, J. J. P.; Pople, J. A. Gaussian 92/DFT; Gaussian Inc., Pittsburgh, PA, 1993.

(38) Allinger, N. L. mm3(92); QCPE, Bloomington, IN, 1992.

(39) Allinger, N. L.; Yuh, Y. H.; Lii, J. H. *J. Am. Chem. Soc.* **1989**, *111*, 8551.

(40) Rappé, A. K.; Casewit, C. J.; Cowell, K. S.; Goddard, W. A., III; Skiff, W. M. *J. Am. Chem. Soc.* **1992**, *114*, 10024.